



Cu–Zr and Cu–Zr–Al clusters: Bonding characteristics and mechanical properties

Ch.E. Lekka*

University of Ioannina, Department of Materials Science and Engineering, Ioannina 45110, Greece

ARTICLE INFO

Article history:

Received 30 July 2009

Received in revised form

26 December 2009

Accepted 10 February 2010

Available online 18 February 2010

Keywords:

Clusters

Metallic glasses

Density functional theory

Electronic structure

ABSTRACT

We present density functional theory (DFT) calculations results on two representative clusters (Cu_7Zr_6 and $\text{Cu}_{10}\text{Zr}_5$) and their interconnections (touching and interpenetrating). The choice of these clusters and their combinations is dictated from previous molecular dynamics (MD) simulations results on the $\text{Cu}_{60}\text{Zr}_{40}$ model metallic glass (MG) in which they were found to be the most abundant microstructural units. In addition, aiming in gaining inside on the experimental findings referring to properties improvement upon small Al additions in the CuZr MGs, we performed calculations for the same systems in which Al substitutional atoms were incorporated into the clusters. In all cases the electronic structures were analyzed and the corresponding bonding characteristics were deduced. Moreover, in order to reveal the electronic modifications these systems subsist under mechanical deformation, we performed non-equilibrium calculations by applying tensile solicitations and we deduced the basic alterations that are responsible for the systems' responses. It turns out that Al has elemental bonding preference; its presence in the clusters and in their interconnections alters significantly their electronic structure by introducing new low-energy states, while significant charge transfer occurs upon mechanical deformation. The present results are in line with the available experimental findings and provide inside on the fundamental issues that are related with the improvement of the glass forming ability and of the mechanical properties in the systems that contain small Al additions.

© 2010 Elsevier B.V. All rights reserved.

1. Introduction

The Cu–Zr bulk metallic glasses (MG) exhibit good mechanical properties but usually macroscopic lack of ductility. This is due to the localization of shear into very thin bands, approximately of 10 nm large that are formed through the interconnection of the shear transformation zones (STZ). It is suggested that the STZ consist of tiny icosahedral-like clusters (ICOs) that respond spontaneously in the applied stress and reorganize their positions through cooperative movements [1–14]. Furthermore, it is experimentally found that Al additions in the Cu–Zr MGs improve the system's macroscopic plasticity, the glass forming ability, while they induce a hardening-like behavior [15–18]. In addition, very recent density functional theory calculations on Cu–Zr–Al system revealed that a small percentage of Al in this ternary MG leads to dramatically increased population of full icosahedra and their spatial connectivity compared to the Cu–Zr based binary. It was also suggested that the stabilization effect of Al is not merely topological, but it is originated from the electronic interactions and the resulting bond shortenings [19]. The latter could be explained by the covalent-like bonding of Al central atom with Cu or Zr shell atoms of ICO-like

clusters found by other density functional calculations [20]. Nevertheless, the role of Al in the structural and electronic properties of CuZr ICO-like clusters for several cluster's sites has still not investigated akin with their role in the properties of interpenetrating clusters.

In the present work density functional theory calculations (DFT) were performed aiming in revealing the influence of Al additions in the structural and electronic properties of ICO-like clusters found in the $\text{Cu}_{60}\text{Zr}_{40}$ system [7] at equilibrium and upon 10% tensile deformation. The study focuses on the bonding characteristics that Al introduces in the ICO clusters upon substitution of shell atoms or additions, while the work is also extended to selective interpenetrating ICO clusters.

2. Computational details

Standard Kohn–Sham self-consistent density functional theory method in the local density approximation was used by means of the SIESTA code. Core electrons were replaced by norm-conserving pseudo-potentials [21] in the fully non-local Kleinman–Bylander [22] form and the basis set is a general and flexible linear combination of numerical atomic orbitals (NAOs) constructed from the eigenstates of the atomic pseudo-potentials [23]. The non-local partial-core exchange–correlation correction was included for Cu to improve the description of the core–valence interactions [24,25].

* Tel.: +30 26510 07310.

E-mail address: chlekka@cc.uoi.gr.

The Zr pseudo-potential was calculated for the Zr^{2+} ion case and found to obtain generally satisfactory results for the metallic Zr [26]. An auxiliary real space grid equivalent to a plane-wave cutoff of 100 Ry was used, while for the geometry optimization, the structure is considered fully relaxed when the magnitude of forces on the atoms is smaller than 0.04 eV/Å.

3. Results and discussion

Let us first consider the cases of a 13-atom Cu-centered icosahedral Cu_7Zr_6 and a 15-atom Zr-centered ICO-like, which is slightly bigger (rhombic dodecahedron (RD)), the $Cu_{10}Zr_5$ cluster, to subsequently tackle their combinations, i.e. when they are interpenetrating with another Zr-centered ICO cluster, namely the $Cu_{10}Zr_3$ or a Cu-centered RD cluster, the Cu_9Zr_6 , respectively. This choice was dictated by the findings of previous MD simulations of the $Cu_{60}Zr_{40}$ MG [7]. For the Al-rich systems, the cases of Al substitution of the cluster's centered or shell atom (Cu or Zr) as well as the case of addition of an Al atom were considered.

Fig. 1a depicts the electronic density of states (EDOS) for the Cu_7Zr_6 pure cluster (black line), along with the cases of the same cluster but with Al addition (purple line), Al substitutions of the Cu-centered atom (red line), the Cu shell atom (blue line) and the Zr shell atom (green line). The insets depict schematic representations of these clusters. It is easily seen a main band from -4 eV up to -2 eV that is principally due to Cu atoms, while the Zr atoms are mainly responsible for the states that are close to the Fermi level [20]. The two sharp lowest energy peaks of Cu_7Zr_6 around -6.1 eV and -5.4 eV are due to the Cu-central atom, while the Al presence introduces new lower energy states, the effect being more pronounced in the cases of substitution of the central atom and Zr cell atom. It is worth to be noted that in the case of Al-centered clusters, the energy state around -5.4 eV is absent, an observation that is consistent with the fact that these states are originated from the Cu-central atom. In the pure $Cu_{10}Zr_5$ case (black line), Fig. 1b, the Cu shell atom energy band is wider, while the lowest energy state (-5.9 eV) is now closer to the Fermi level by 0.2 eV, compared to the Cu_7Zr_6 pure case. In general, the Cu-centered clusters exhibit a

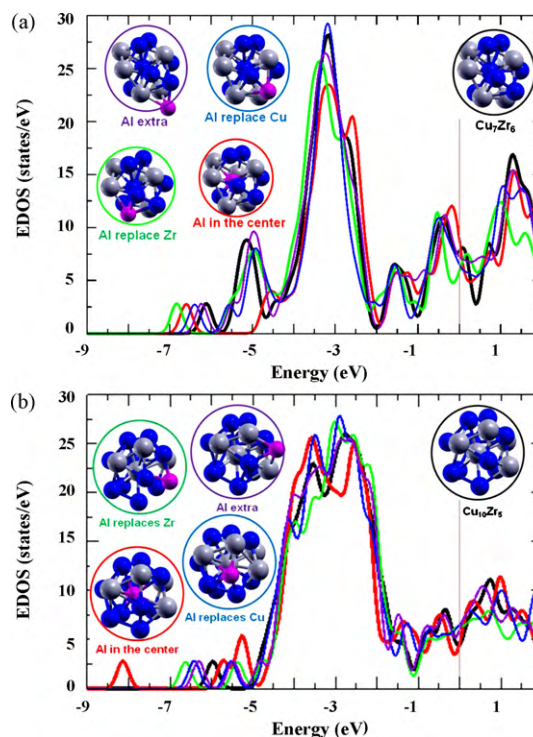


Fig. 1. EDOSs for (a) the Cu_7Zr_6 and (b) the $Cu_{10}Zr_5$ single cluster cases at equilibrium. Black line stands for the pure case, purple line for the case of Al addition, while the substitutions of the Cu-centered and shell atom by Al are represented by red and blue lines, respectively. The contributions of the Zr cell atoms are given by the green line. (For interpretation of the references to color in the figure caption, the reader is referred to the web version of the article.)

state around -5 eV, whereas the lowest peak is always due to the central atom (Cu or Zr). The Al presence modifies the energy states below -4 eV. The Al induces new states in the lowest energies (-8.15 eV), while new states appear around -5.7 eV, similarly to the Cu-centered cases, Fig. 1a. In the other Al containing cluster

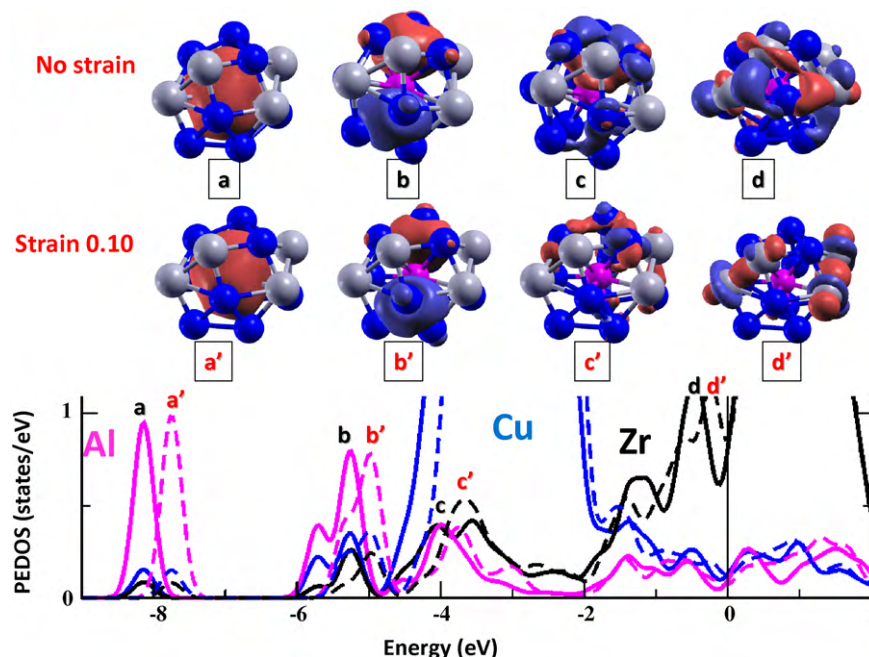


Fig. 2. PEDOS of the Al-centered $Cu_{10}Zr_5$ RD clusters at equilibrium and under tensile deformation, solid and dashed lines, respectively. The colors purple, blue and black stand for the Al, Cu and Zr. In the insets the cluster's wavefunctions at selective a (a'), b (b'), c (c') and d (d') energy states at equilibrium (upon 10% tensile deformation), respectively are also given. (For interpretation of the references to color in the figure caption, the reader is referred to the web version of the article.)

cases (Al addition or shell-atom substitution), the new lowest energy states stand within the single Cu–Zr clusters and the Al-centered cluster cases. Summarizing, the presence of Al atoms introduces new well localized energy states in lower energies than the Cu or Zr atoms, suggesting stronger interatomic interactions.

Fig. 2 depicts the partial electronic density of states (PEDOS) for the $\text{Cu}_{10}\text{Zr}_5$ with Al central atom at equilibrium (solid lines) and upon deformation (dashed lines), referring to the Al (purple line), Cu (blue line) and Zr atom (black line). For selective energy states we also show the cluster's wavefunctions (blue and red areas correspond to the corresponding negative and positive sign). It comes out that in all cases the mechanical deformation induces a small shift (~ 0.2 eV) towards the Fermi level, which is more pronounced in the cases of clusters containing Al, states (a) and (b) in Fig. 2. Close inspection of the wavefunctions in the (a) state revealed a covalent-like bonding between the Al s and the shell Cu d elec-

trons, while in the (b) state the Al p electrons are mainly involved. Very interestingly, both states remain intact after the application of tensile deformation. In addition, the states from -4 eV up to -2 eV are dominated by localized Cu shell atoms energy states (energy states c), while the states close to the Fermi level (e.g. state d) are characterized by d–d bonding between the Zr shell atoms. Upon deformation these energy states are depleted through a small charge transfer towards the deformed cluster's edges.

Fig. 3a illustrates the EDOSs for the $\text{Cu}_{12}\text{Zr}_{10}$ supercluster that consists of two interpenetrating Cu-centered ICO clusters (blue line) [27], along with the same quantities corresponding to the case of (a) substitution of the central atom of one of the ICO clusters by Al (red line), (b) the substitution of a Cu (purple line) or Zr common neighbor atom (light blue line), as well as (c) the case of Al addition (green line). The main features of the EDOS are similar with the pure Cu-centered ICO cluster, Fig. 1a, while the Al substitution/addition

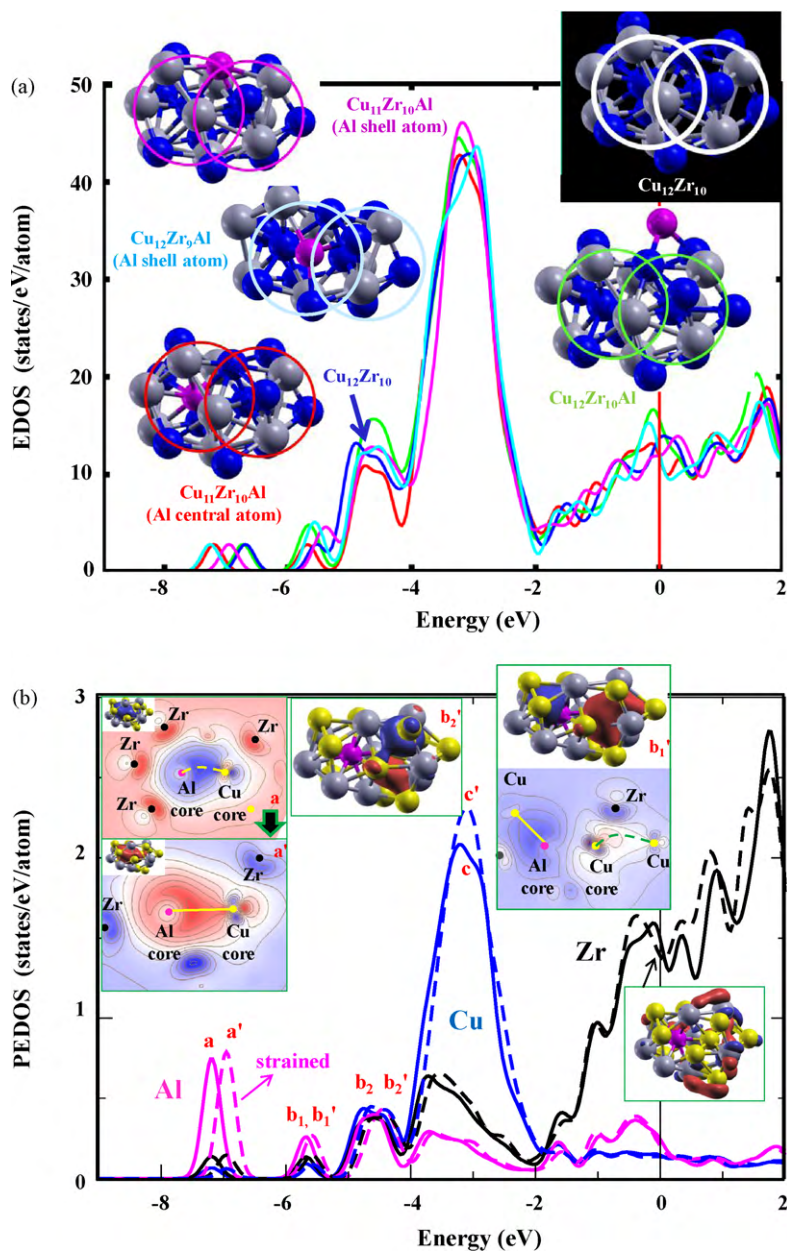


Fig. 3. (a) EDOSs $\text{Cu}_{12}\text{Zr}_{10}$ supercluster at equilibrium: for the pure case (black line), the Al addition (green line) and the Al substitutions of: the Cu-centered atom (red line), the Cu shell atom (purple line) and the Zr shell atom (blue line). (b) PEDOS of the Al-centered atom at equilibrium (solid lines) and upon 10% tensile deformation (dashed lines). Al, Cu and Zr PEDOSs are given with magenta, blue and black lines. (For interpretation of the references to color in the figure caption, the reader is referred to the web version of the article.)

mainly influences the lowest energy states. Given that now we are dealing with two clusters and therefore two central atoms, the Cu-centered atom energy state around -5 eV remains even upon Al substitution of one of the central atoms, while Al addition in the $\text{Cu}_{12}\text{Zr}_{10}$ does not alter the main EDOS's features at lowest energy states, influencing mainly the EDOS between -5 eV and -3 eV. In agreement with Figs. 1 and 2, the Cu shell atoms are responsible for these energy states and the Al atom prefers to bond with these atoms rather than with the Zr shell atoms. From all cases, in Fig. 3b the PEDOS of the substitution case referring to the Al central atom is selected. It can be seen that upon deformation, a small shift (~ 0.5 eV) is visible for the lowest energy states (a-state) (around -7 eV) that are introduced by the presence of Al (magenta line). Interestingly, all the other energy states are not shifted upon deformation. From the detailed inspection of the wavefunctions at state (a) it worth's to be noted a directional covalent-like bonding between the Al s and Cu d central atoms. For this interaction it came out that the electronic distribution and the bonding character is not altered upon 10% tensile deformation (state a'). In addition, in the b_1 energy state both central atoms participate forming covalent-like bonding with the Cu shell atoms, while in the b_2 energy state d–d bonding between the Cu-central atom and the Cu shell atoms dominate. Finally, the highest occupied cluster's orbital is characterized by the Zr–Zr shell atom or Zr–Cu shell bonding.

4. Conclusions

This communication is devoted in the study of the influence of the presence of Al atoms in representative Cu–Zr ICO or RD clusters, including a case of two interpenetrating clusters, i.e. two Cu-centered ICO-RD clusters. It was found that in all cases the central atoms are responsible for the lowest energy states, the states between -2 eV and -4 eV are mainly due to Cu–Cu shell atoms, while the Zr shell atoms are responsible for the energy states close to the Fermi level. In addition, it came out that the presence of an Al atom in the Cu–Zr clusters introduces new well localized states at low energies that are characterized by covalent-like bond, thus suggesting better mechanical properties. Finally, it was found that in all

cases studied the mechanical solicitation results in selective shifts of the EDOSs towards lower energy levels, the effect being more pronounced in the cases of Al substitutions. The present results can provide inside in the understanding of the fundamental issues that are related with the experimental findings concerning the GFA and mechanical properties improvement upon small Al additions in Cu–Zr metallic glasses and could be used for the design of new MGs with tailored functionalities.

References

- [1] F. Spaepen, Nat. Lond. 408 (2000) 781.
- [2] D.B. Miracle, Nat. Mater. 3 (2004) 697.
- [3] Ch.E. Lekka, A. Ibenskas, A.R. Yavari, G.A. Evangelakis, Appl. Phys. Lett. 91 (2007) 214103.
- [4] H.W. Sheng, Y.Q. Cheng, P.L. Lee, S.D. Shastri, E. Ma, Acta Mater. 56 (2008) 6264.
- [5] X.D. Wang, S. Yin, Q.P. Cao, J.Z. Jiang, Appl. Phys. Lett. 92 (2008) 011902.
- [6] M. Wakeda, Y. Shibutani, S. Ogata, J. Park, Intermetallics 15 (2007) 139.
- [7] A.E. Lagogianni, G.A. Almyras, Ch.E. Lekka, G.A. Evangelakis, J. Alloys Compd 483 (2009) 658.
- [8] R.S. Liu, K.J. Dong, J.Y. Li, A.B. Yu, R.P. Zou, J. Non-Cryst. Solids 351 (2005) 612.
- [9] C.A. Schuh, A.C. Lund, Nat. Mater. 2 (2003) 449.
- [10] A.R. Yavari, Nat. Lond. 439 (2006) 405.
- [11] R.D. Conner, W.L. Johnson, N.E. Paton, W.D. Nix, J. Appl. Phys. 94 (2003) 904.
- [12] C.A. Schuh, A.C. Lund, T.G. Nieh, Acta Mater. 52 (2004) 5879.
- [13] A.R. Yavari, J.J. Lewandowski, J. Eckert, MRS Bull. 32 (2007) 635.
- [14] H. Guo, P.F. Yan, Y.B. Wang, Z.F. Zhang, J. Tan, M.L. Sui, E. Ma, Nat. Mater. 6 (2007) 73.
- [15] J. Das, M.B. Tang, K.B. Kim, L.R. Theissmann, F. Baier, W.H. Wang, J. Eckert, PRL 94 (2005) 205501.
- [16] K.B. Kim, J. Das, F. Baier, M.B. Tang, W.H. Wang, J. Eckert, APL 88 (2006) 051911.
- [17] J. Das, K.B. Kim, W. Xu, B.C. Wei, Z.F. Zhang, W.H. Wang, S. Yi, J. Eckert, Mater. Trans. 47 (2006) 2606.
- [18] J. Das, S. Pauly, C. Duhamel, B.C. Wei, J. Eckert, J. Mater. Res. 22 (2007) 326.
- [19] Y.Q. Cheng, H.W. Sheng, E. Ma, PRL 102 (2009) 245501.
- [20] Ch.E. Lekka, G.A. Evangelakis, Scr. Mater. 61 (2009) 974.
- [21] N. Troullier, J.L. Martin, Phys. Rev. B43 (1991) 1993.
- [22] L. Kleinman, D.M. Bylander, Phys. Rev. Lett. 48 (1982) 1425.
- [23] E. Artacho, D. Sanchez-Portal, P. Ordejon, A. Garcia, J.M. Soler, Phys. Status Solidi B215 (1999) 809.
- [24] S.G. Louie, S. Froyen, M.L. Cohen, Phys. Rev. B 26 (1992) (1738).
- [25] J. Junquera, O. Paz, D. Sanchez-Portal, E. Artacho, Phys. Rev. B 64 (2001) 235111.
- [26] J.-P. Crocombette, D. Ghaleb, J. Nucl. Mater. 257 (1998) 282.
- [27] G.A. Almyras, Ch.E. Lekka, N. Mattern, G.A. Evangelakis, Scr. Mater. 62 (2010) 33.